Inhibition and modulation of rhythmic neuronal spiking by noise

Henry C. Tuckwell and Jürgen Jost
Max Planck Institute for Mathematics in the Sciences, Inselstr. 22, 04103 Leipzig, Germany

Boris S. Gutkin
Group for Neural Theory, Département des Etudes Cognitives, Ecole Normale Supérieure, 5 rue d'Ulm, 75005 Paris, France

(Received 24 December 2008; revised manuscript received 11 June 2009; published 18 September 2009)

We investigated the effects of noise on periodic firing in the Hodgkin-Huxley nonlinear system. With mean input current μ as a bifurcation parameter, a bifurcation to repetitive spiking occurs at a critical value $\mu_c \approx 6.44$. The firing behavior was studied as a function of the mean and variance of the input current, firstly with initial resting conditions. Noise of a small amplitude can turn off the spiking for values of μ close to μ_c, and the number of spikes undergoes a minimum as a function of the noise level. The robustness of these phenomena was confirmed by simulations with random initial conditions and with random time of commencement of the noise. Furthermore, their generality was indicated by their occurrence when additive noise was replaced by conductance-based noise. For long periods of observation, many frequent transitions may occur from spiking to nonspiking activity when the noise is sufficiently strong. Explanations of the above phenomena are sought in terms of the underlying bifurcation structure and the probabilities that noise shifts the process from the basin of attraction of a stable limit cycle to that of a stable rest state. The waiting times for such transitions depend strongly on the values of μ and σ and on the forms of the basins of attraction. The observed effects of noise are expected to occur in diverse fields in systems with the same underlying dynamical structure.

DOI: 10.1103/PhysRevE.80.031907 PACS number(s): 87.19.lc, 05.40.−a

I. INTRODUCTION

Models for nerve cell activity often take the form of a nonlinear system of differential equations [1]. The effects of noise on such dynamical systems have been investigated with many models and preparations [2–11]. In the majority of cases, the effects have been facilitatory; that is, neurons tend to fire more rapidly when their input processes have a stochastic component [12–14], even if the latter has zero mean [15]. In some cases, there is a maximal response at a particular noise level—a phenomenon called *stochastic resonance,* which arises in several biological and other applications [16–22]. This may occur even when the input signal is nonperiodic [23] or without external forcing [24]. Of interest also is the phenomenon of coherence resonance [25,26], which has been studied for noise-induced firing in a Hodgkin-Huxley model with Ornstein-Uhlenbeck synaptic input [28].

In recent articles [27,29,30], we have reported and analyzed a case where noise, instead of having a facilitatory effect, could inhibit the spiking activity of coupled pairs of type 1 [31,32] model neurons, typified by quadratic integrate and fire (or theta-neuron) model cells [1,32]. Here, we report on the occurrence of the inhibitory effects of noise on spiking activity in a single (type 2) Hodgkin-Huxley (HH) model neuron. This model, which consists of a system of four ordinary (or partial) differential equations, is basic in neurophysics as it was the first to provide a theoretical framework for action potentials or spikes. Thenceforth, it has often been employed to ascertain the effects of noise on spiking activity [5,13,26,28,41].

The inputs we consider are both of the additive current type, with fixed and random initial conditions, and the conductance type. When the HH neuron is driven by mean currents close to the critical value for the onset of repetitive firing, a small amount of noise can dramatically reduce the firing activity. This phenomenon has indeed been hinted at experimentally [33]. In addition, we have found that there is a minimum in the firing rate at a particular noise amplitude. Additionally, we briefly consider long-term periods of noise, which, particularly when the noise amplitude is large, may lead to rapid intermittent switching from spiking to nonspiking states.

II. HH NEURONS WITH ADDITIVE NOISE

For a single space-clamped HH-model neuron [34] with additive (or "current") noise we have for the depolarization $V(t)$ at time t

$$dV = \frac{1}{C}[\{\mu + \bar{g}_K n^4(V_K - V) + \bar{g}_{Na} m^3 h(V_{Na} - V) + g_L(V_L - V)\}dt + \sigma dW], \tag{1}$$

and for the dimensionless auxiliary variables

$$dn = [\alpha_n(1-n) - \beta_n n]dt \tag{2}$$

$$dm = [\alpha_m(1-m) - \beta_m m]dt \tag{3}$$

$$dh = [\alpha_h(1-h) - \beta_h h]dt, \tag{4}$$

where C is the membrane capacitance per unit area, μ, which may depend on t, is the mean input current density, $\bar{g}_K$, $\bar{g}_{Na}$, and g_L are the maximal (constant) potassium, sodium, and leak conductances per unit area with corresponding equilibrium potentials V_K, V_{Na}, and V_L, respectively. The noise enters as the derivative of a standard Wiener process W and has amplitude σ. The auxiliary variables are $n(t)$, the potassium

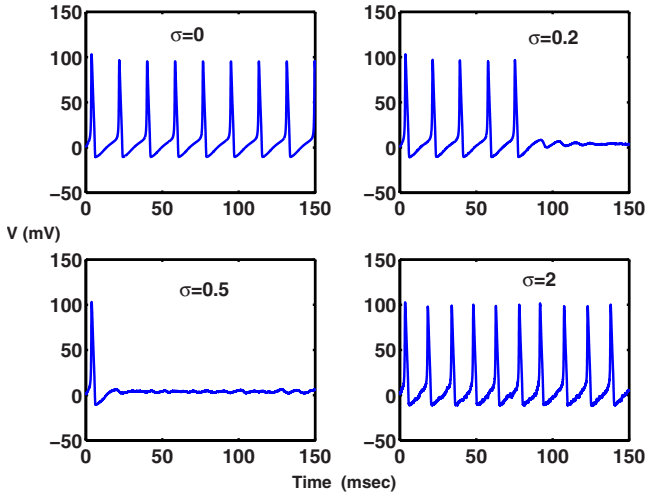

FIG. 1. (Color online) Showing voltage trajectories with spikes for a current-driven Hodgkin-Huxley model neuron. The mean input current density μ is 6.6 μA/cm^2 and three examples of the effects of noise of various magnitudes, σ, are shown. Neuron is initially at rest.

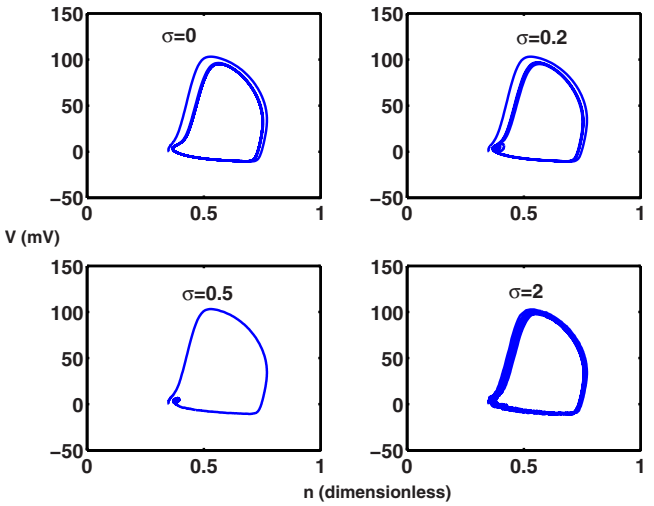

FIG. 2. (Color online) Orbits of voltage versus potassium activation variable corresponding to the plots of Fig. 1. The limit cycle is clearly seen in the noise-free case and the manner in which small noise, σ=0.2, and intermediate noise, σ=0.5 may switch the orbit away from the limit cycle. When σ=2, the orbits are close to the noise-free case.

activation, $m(t)$, the sodium activation, and $h(t)$, the sodium inactivation. The coefficients in the differential equations for the auxiliary variables as functions of depolarization are

$$\alpha_n(V) = \frac{10 - V}{100[e^{(10-V)/10} - 1]}, \quad \beta_n(V) = \frac{1}{8}e^{-V/80}$$

$$\alpha_m(V) = \frac{25 - V}{10[e^{(25-V)/10} - 1]}, \quad \beta_m(V) = 4e^{-V/18}$$

$$\alpha_h(V) = \frac{7}{100}e^{-V/20}, \quad \beta_h(V) = \frac{1}{e^{(30-V)/10} + 1}.$$

These equations were used to simulate spike trains in a single HH neuron with various values of the mean input current μ and for various values of the noise amplitude σ. The following standard parameter set was employed: C=1, $\bar{g}_K$=36, $\bar{g}_{Na}$=120, g_L=0.3, V_K=−12, V_{Na}=115, and V_L=10. The standard initial values are $V(0)$=0, $n(0)$=0.35, $m(0)$=0.06, and $h(0)$=0.6. The units for these various quantities are as follows: all times are in msec, all voltages are in mV, all conductances per unit area are in mS/cm^2, C is in μF/cm^2, μ is in μA/cm^2, and σ is in μA msec$^{1/2}$/cm^2.

III. RESULTS

When there is no noise and μ is less than a critical value μ_c, only subthreshold responses occur. However, as μ increases past the bifurcation value $\mu_c \approx 6.44$, a stable and unstable limit cycle appear so that repetitive periodic spiking occurs. The simulation results we obtained showed clearly that, for μ in the vicinity of μ_c, the expected number of spikes at first drops as the noise strength goes up and then starts to increase. Figure 1 shows the voltage responses of the model neuron in the current-driven case with various noise levels for μ=6.6. Without noise (top left record), there is a repetitive stream of output spikes, there being 8 in the time period of duration 150 msec shown. As expected, adding noise makes the output spike times irregular.

In this situation, extremely weak noise naturally has little effect. Unexpectedly, slightly larger amounts can have a significant inhibitory effect on the neuron's spiking activity. Moreover, moderate amounts of noise can actually stop the spiking for a long time. In the examples shown, a noise level of σ=0.2 can halt the firing of action potentials after five spikes and a somewhat larger noise level of σ=0.5 here stops the spiking after just one spike. When the noise level is turned up to σ=2, more spikes are emitted, there being 10 in the trial shown. In Fig. 2 are shown plots of voltage versus the potassium conductance variable, n. These phase-space diagrams, which show the collapse of the limit cycle, are useful in understanding the effects of noise of various levels, as discussed below. Note that in all cases, if noise is present, it is on at and after t=0, except in the case where as reported in Fig. 7, it is switched on at a random time.

As it was at first surprising to encounter a minimum in the number of spikes as noise level increased, we simulated the firing activity for many values of μ and σ with results as given in Figs. 3 and 4, where the mean spike counts are shown for 200 trials, for $\mu \leq 6.4$ (Fig. 3) and for $\mu \geq 6.44$ (Fig. 4), respectively. In Fig. 3 it can be seen for the smaller values of the mean input current (μ=4 to just less than 6) the spike counts monotonically increase from zero as the noise strength increases.

When however μ gets close to and just above μ_c, small noise has a noticeably depressing effect on the spiking and there appears a minimum in the mean spike count as σ increases. As seen in Fig. 4, as μ increases through μ_c, the minimum at small values of σ becomes more and more pronounced. In each case when the noise is large enough, beyond the minimum, the mean spike count increases monotonically. However, as is to be expected, when μ is

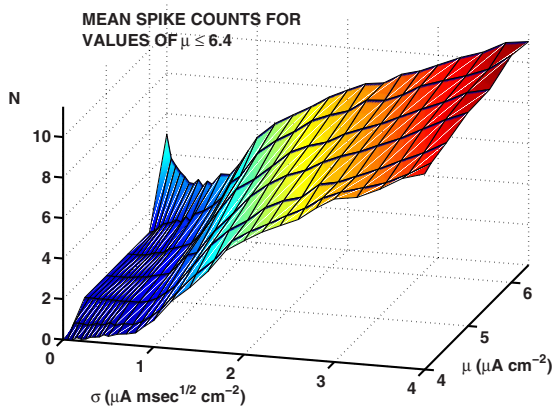

FIG. 3. (Color online) Mean numbers of spikes in an HH neuron over a 150-msec period at various values of the mean input strength $\mu < \mu_c$ and for various noise levels, σ. Neuron initially at rest. Based on 200 trials.

sufficiently large, the strong current overrides any effects that noise may have, and the phenomenon eventually disappears. Furthermore, there is a second bifurcation point, μ_c^* at which the equilibrium point loses stability so that noise can no longer drive the system from a limit cycle to a nonspiking state. Simulations (not shown) confirm that the minimum is rather shallow beyond $\mu=8$ and has disappeared at $\mu=12$. In approximate terms, the drop in observed spike count (in 150 msec) with noise relative to the zero noise spike count jumps from 0 to 48% near $\mu=6.4$, where only transient responses occur without noise, and achieves a maximum of 67% near $\mu=\mu_c$.

To further illustrate these effects, we show in Fig. 5 the mean spike numbers as a function of noise level over a 1000 msec time interval (100 trials) for three values of μ, below μ_c, just above μ_c, and considerably above μ_c. The minimum near $\sigma=0.4$ is clearly seen for $\mu=6.8$ and is even more pronounced than it was for the case of a 150 msec observation period. At the minimum, the mean number of spikes is only about 6, representing a drop in mean spike count of 89% relative to the noise-free case. For larger σ, the mean number

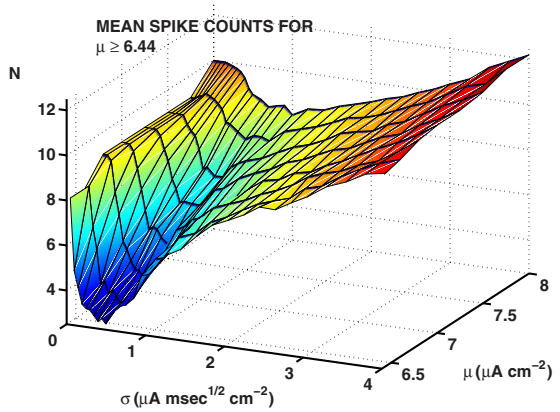

FIG. 4. (Color online) Mean numbers of spikes in an HH neuron over a 150-msec period at various values of the mean input strength $\mu \geq \mu_c$ and for various noise levels, σ. Neuron initially at rest. Based on 200 trials.

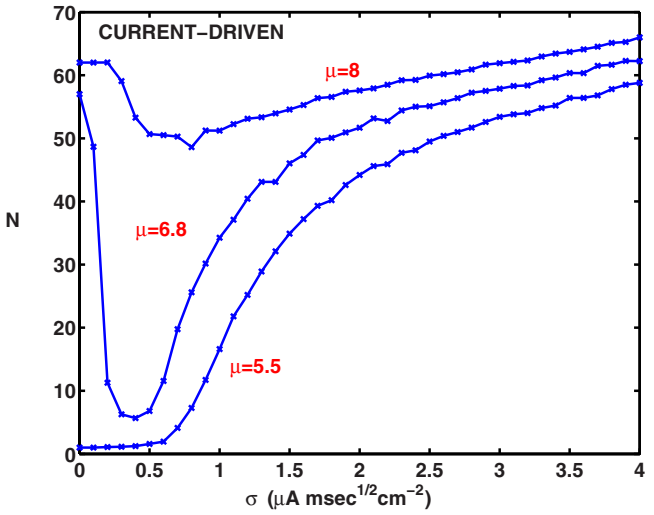

FIG. 5. (Color online) Mean numbers of spikes (100 trials) versus noise level in the single HH-model neuron for a 1000-msec time interval with additive input current for three mean current strengths as indicated. Neuron initially at rest.

of spikes increases at first quite sharply and then more slowly as the noise level increases. For the larger value of the mean input current, $\mu=8$, there are 62 spikes without noise and a noticeable, yet less pronounced, minimum of value 48 in the mean number of spikes when σ is just less than 1. For $\mu=5.5$, before the onset of rhythmic spiking, the mean spike count increases seemingly monotonically as the noise level increases. Note that noise may destroy the regular nature of the spike train when $\mu > \mu_c$.

A. Random initial conditions

The results described above, and particularly in Figs. 3–5, were obtained with initial conditions, which were the same on each trial, being the standard resting values for V, n, m, and h. Note that by definition [34], the rest state of a neuron corresponds to depolarization, $V=0$. In order to see if the observed phenomena were somehow a consequence of this special choice of initial data, simulations were performed, over a 500 msec interval, in which the values of $V(0)$, $n(0)$, $m(0)$, and $h(0)$ were chosen randomly. The value of $V(0)$ was uniformly distributed over $(-10.5, 103.3)$, which gives the approximate range of values of V during rhythmic spiking. The values of $n(0)$, $m(0)$, and $h(0)$ were uniformly distributed $U(0,1)$ random variables. Three values of μ, those as in Figure 5, were employed, and 23 values of σ, namely, $0.1, \ldots, 1.0, 1.2, \ldots, 2.0, 2.25, \ldots, 4.0$. The results are shown in Fig. 6. Firstly, the mean spike counts over all (200) trials are shown as the solid (blue) curve and crosses. However, when initial data are chosen randomly, sometimes the initial value falls in the basin of attraction B_r of the stable equilibrium point and sometimes in that, B_s, of the limit cycle. Note that both of these sets, B_r and B_s, depend on μ. The estimated probabilities, based on 4600 cases, that the initial point $[V(0), n(0), m(0), h(0)]$ fell in B_r, are 0.683, 0.161, and 0.067 for $\mu=5.5$, 6.8 and 8, respectively. The (red) dashed curves and circles are the mean spike counts when the pro-

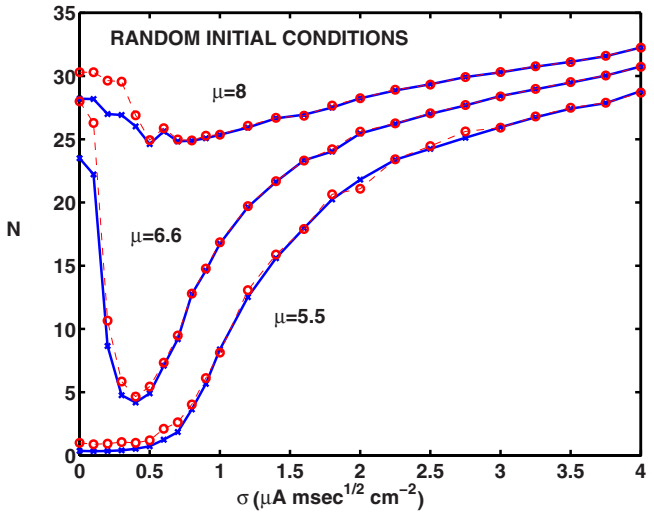

FIG. 6. (Color online) Mean spike counts in a 500-msec time interval for an HH neuron with random initial conditions for all four components as described in the text. Here, the noise is additive (current noise). Values of mean input current μ and noise amplitude σ as indicated. The solid (blue) lines and crosses are for the whole sample of 200 initial values. The dashed (red) line and the circles are the results only for those initial points that fell in the basin of attraction of the limit cycle. Note that the time interval here is one half of that in Figs. 5 and 10, resulting in about half as many spikes.

cess starts in B_s. It can be seen that the results for the mean spike counts versus σ parallel those for the case of a fixed initial value set at the rest point whether all results are taken into account or whether the results are restricted to those cases where the initial point was in B_s. When only those cases are taken into account where the initial point is in B_r then for all three values of μ, the mean spike counts increase monotonically from zero to soon approach the curves shown in Fig. 6, in line with the noise-induced nature of these spikes. Since, however, our main concern is with the effects of noise on spiking which is already occurring, it may be concluded that the inhibitory effect of noise illustrated in Figs. 1–5 is robust for random initial conditions which fall within B_s.

B. Switching on the noise at a random time

In the previous subsection, random initial data were employed, but on a few occasions, no spikes ensued in a 500 msec time period. In order to examine the effects of noise on rhythmic spiking when the latter is already present, the noise was switched on at a random time and the effects on spiking activity noted. For the two values of μ, 6.8, and 8.0, which are greater than μ_c, and values of σ in (0,2], the HH neuron model was driven by the deterministic component only up to $t=100$ msec, by which time rhythmic spiking was established. The noise was switched on at the random time T_R which was uniformly distributed on the interval (100, 120), which contains one complete period of spiking. Illustrative spike trains are shown in Fig. 7(a). The mean number N^* (the mean of a different random variable from previously) of spikes in the interval $(T_R,500)$ was determined and the results are shown in Fig. 7(b). The dependence of N^* on σ for each value of μ parallels that obtained in Fig. 5 (fixed initial data) and Fig. 6 (random initial data). These results also add credence to the robustness of the phenomena described above.

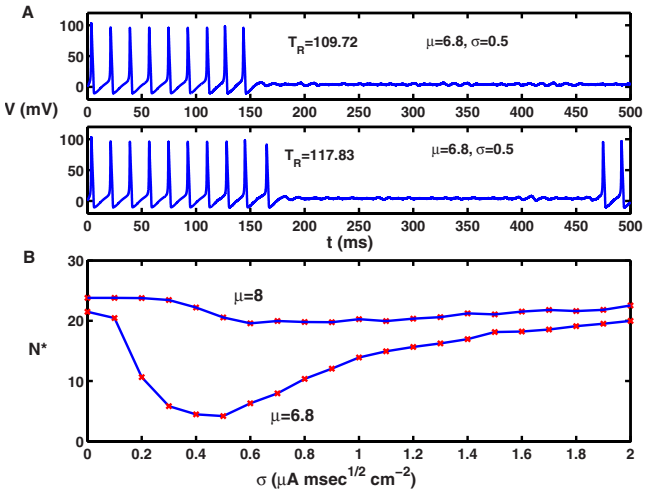

FIG. 7. (Color online) Rhythmic spiking with additive noise switched on at a random time. (A) Showing two sample paths with $\mu=6.8$ and $\sigma=0.5$. The noise component of the input is switched on randomly after $t=100$. The time at which the noise is switched on is T_R. See text for details. (B) Mean spike counts N^* (200 trials) in the time period $(T_R,500)$ plotted against noise amplitude σ for two values of $\mu=6.8$ and $\mu=8$, which give rhythmic spiking in the absence of noise. Neuron at rest at $t=0$.

C. Long-term stimulation

The above sets of results were based on either a 150, 500, or 1000 msec time period. For longer observation periods, when σ is large, and μ is in the appropriate range of values, there is a greater chance of alternations between spiking and nonspiking states. An example is shown in Fig. 8 for a

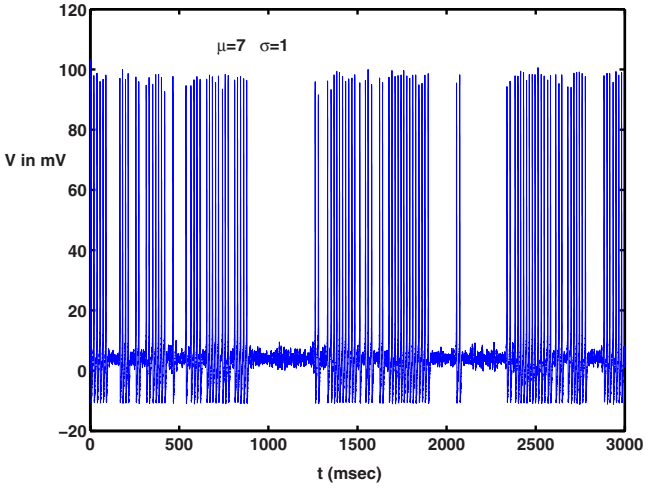

FIG. 8. (Color online) A long-term sample path for V in an HH-model neuron with additive noise: $\mu=7$ and $\sigma=1$. Neuron initially at rest.

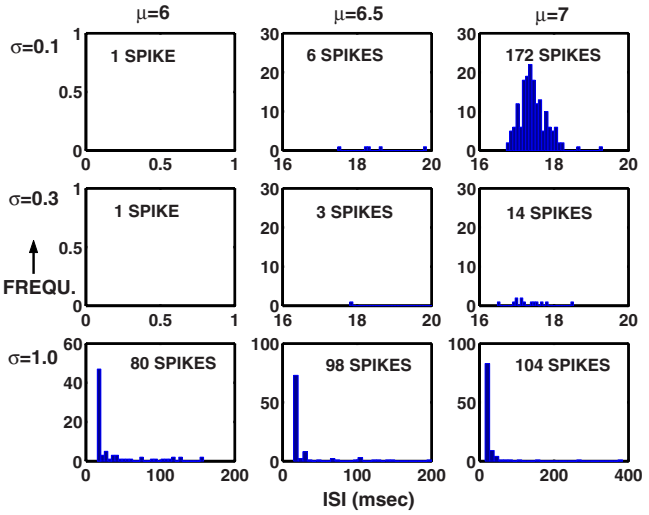

FIG. 9. (Color online) Interspike interval histograms for a 3000-msec time period for three values of μ with small, intermediate, and large noise. The inter-spike intervals are in msec.

current-driven HH neuron with $\mu=7$ and $\sigma=1$ with an observation period of 3000 msec. In this case, there is a total of 104 spikes, which may be compared with 98 for the same noise and $\mu=6.5$ and 80 for $\mu=6$. These and histograms of the interspike interval for sample paths of the same duration and other values of μ and σ are shown in Fig. 9. It can be seen that for a noise level of $\sigma=0.3$, the numbers of spikes with $\mu=6$, 6.5, and 7 are only 1, 3, and 14, respectively. In contrast, when $\sigma=0.1$, there are 1, 6, and 172 spikes, respectively.

IV. HH NEURONS WITH CONDUCTANCE-DRIVEN INPUT

The above effects of noise on the firing of a single HH neuron, including the occurrence of a minimum in the firing activity, were obtained with an additive input current containing both deterministic and random components. Such an input, which approximates current being injected into a cell by microelectrode in a laboratory preparation, is sometimes referred to as current-driven [36]. In order to more closely represent the synaptic input received by real neurons, we include reversal potentials in the synaptic currents applied to our model cell [35,36]. The differential equations for the three auxiliary variables, n, m, and h are unaltered but there are now two subsidiary equations for the excitatory and inhibitory conductances. The differential equation for V contains a current $I_c=g_E(t)(V_E-V)+g_I(t)(V_I-V)$ from excitatory and inhibitory synaptic inputs

$$dV=\frac{1}{C}\{[\bar{g}_K n^4(V_K-V)+\bar{g}_{Na}m^3h(V_{Na}-V)+g_L(V_L-V)]+I_c(t)\}dt \quad (5)$$

$$dg_E=-\frac{1}{\tau_E}[g_E-\bar{g}_E]dt+\sigma_E dW_E(t) \quad (6)$$

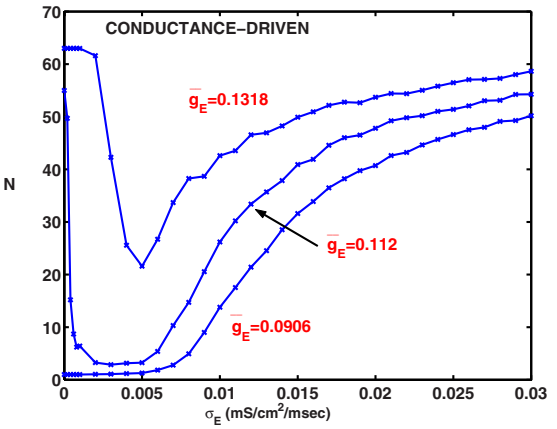

FIG. 10. (Color online) Mean numbers of spikes (100 trials) versus noise level in the single HH-model neuron with conductance-based input current for various conductance strengths as indicated. Observation period 1000 msec. Neuron initially at rest. For parameter values, see text.

$$dg_I=-\frac{1}{\tau_I}[g_I-\bar{g}_I]dt+\sigma_I dW_I(t). \quad (7)$$

Here, $g_E(t), g_I(t)$ are the excitatory and inhibitory conductances per unit area at time t; V_E, V_I, assumed constant but depending on local ion concentrations, are the excitatory and inhibitory synaptic reversal potentials. Furthermore, τ_E, τ_I are time constants, $\bar{g}_E, \bar{g}_I$ are the steady state values of g_E, g_I, and W_E, W_I are standard (independent) Wiener processes that enter with amplitudes σ_E, σ_I. The time constants are in msec and the reversal potentials are in mV. The units for the conductances per unit area are again mS/cm^2 and for σ_E and σ_I the units are mS msec$^{1/2}$/cm^2.

In order to better compare the conductance noise case with that of current noise, we considered excitatory input conductances only. Note that in the diffusion approximation for g_E, when σ_E is large, there may be very occasional excursions of g_E to slightly negative values. In the simulations, however, g_E was restricted to take on only non-negative values. The time constant was set at $\tau_E=2$ msec [36] and $V_E=+80$ mV relative to resting potential. The remaining parameters were chosen to enable a reasonable comparison, in regard to firing behavior, with the additive current case. The excitatory conductance $\bar{g}_E$, which led to repetitive spiking without noise, was very close to a critical value $\bar{g}_{E,c}=0.112$ mS/cm^2. Fig. 10 shows the mean numbers of spikes emitted over a 1000 msec time period at various noise levels for three values of the equilibrium conductance, being less than, approximately equal to, and greater than the critical value for rhythmic spiking.

The bottom curve in Fig. 10 shows the effects of increasing noise when $\bar{g}_E=0.0906$ mS/cm^2, which is below the critical value. With increasing noise levels, the average number of spikes gradually increases from 1 to about 50. When $\bar{g}_E=0.112$ mS/cm^2 and $\sigma=0$, there are 55 spikes in a 1000 msec period. A small amount of noise causes a very large decrease in spike rate and as the noise level increases there is a well-defined minimum at about $\sigma_E=0.004$. For a larger

mean stimulus level, $\bar{g}_E=0.1318$ mS/cm^2, there are 63 spikes without noise. As the noise level increases, a distinct minimum occurs at about $\sigma_E=0.005$. Thus, for both kinds of input current, current-driven and conductance driven, a noise-induced decrease in firing rate occurs for inputs with means near the critical value for periodic spiking and a minimum in spike counts develops as the noise amplitude grows. It is remarkable in the case of conductance-based noise that this inhibitory effect occurs even if the neuron is driven by a purely *excitatory* synaptic input.

V. THEORY

A general qualitative understanding of the weak-noise-induced modification of the periodic activity with appropriate values of μ can be sought in terms of dynamical systems theory and stochastic analysis. The bifurcation structure of the HH dynamical system [37,38] plays an important role in these phenomena as described above. In the absence of noise, regarding μ as the bifurcation parameter, there are three critical values which we denote in increasing order by μ_c, μ_c^*, and μ_c^{**}. For $\mu<\mu_c$ the only stable solution is a rest point, and in this region only a transient response, resembling damped spikes, obtains. Note that in this discussion, we refer to the stable equilibrium as a rest point, which is not, except when $\mu=0$, the physiological rest point at which $V=0$. At μ_c a stable and unstable limit cycle appear by a saddle-node bifurcation. At μ_c^* the unstable limit cycle coalesces with the rest point via a subcritical Hopf bifurcation, destabilizing the rest point. In the range $\mu_c<\mu<\mu_c^*$, where a stable rest point and a stable limit cycle coexist, noise or other types of perturbation may drive the system from one stable solution to the other, which is the basis of the inhibitory effect of noise on rhythmic spiking. For $\mu>\mu_c*$, however, such transitions are not expected, but further analysis is required. Eventually, at $\mu=\mu_c^{**}$ the stable limit cycle coalesces with the unstable rest point so that for $\mu>\mu_c^{**}$ only a stable rest point remains.

Thus, there are two main factors underlying the behavior of the stochastic system, namely, the tendency for noise to drive a neuron to firing when it would not spike without noise (when for the current-driven neuron $\mu<\mu_c$) and the ability of noise to drive the system to and from a (spiking) limit cycle to the rest point when $\mu_c<\mu<\mu_c^*$.

Let $\mathbf{x}$ stand for the collection of backward variables for (V,n,m,h). Assuming that μ is in the range where the system is bistable, the explanations of the different firing behaviors with increasing noise, and indeed the results of Figs. 3–7 and 10, lie in the probabilities $p_{sr}(\mu,\sigma;\mathbf{x})$ and $p_{rs}(\mu,\sigma;\mathbf{x})$ that the process makes a transition from one to the other of two basins of attraction, one being B_s, that of the limit cycle and the other being B_r for the rest state. Note that, strictly speaking, the concept of basin of attraction here refers to the system without noise, because when the dynamical system is random, a clearly defined basin of attraction does not exist as in the deterministic case. Furthermore, the sets B_r and B_s depend on μ.

The probabilities $p_{sr}(\mu,\sigma)$ and $p_{rs}(\mu,\sigma)$ satisfy the partial differential equations [39]

$$Lp_{sr}=0, \quad \mathbf{x}\in B_s, \tag{8}$$

$$Lp_{rs}=0, \quad \mathbf{x}\in B_r, \tag{9}$$

with $p_{sr}=1$ and $p_{rs}=1$ on the respective boundaries. Here, L is the (linear) infinitesimal operator for the HH system. In the case of current noise this operator was given in [40,41] and for the conductance-based noise model it is given in the Appendix as L^*. The solutions of these equations are easily seen to be $p_{sr}=1$ and $p_{rs}=1$ throughout B_s and B_r, respectively (cf. [29]). That is, noise must eventually either turn off the spiking or turn it on. However, the expected values f_{sr} and f_{rs} of the times of exit from B_s and B_r, which can be obtained as solutions of the partial differential equations

$$Lf_{sr}=-1, \quad \mathbf{x}\in B_s, \tag{10}$$

$$Lf_{rs}=-1, \quad \mathbf{x}\in B_r, \tag{11}$$

with zero values on the boundaries of the respective regions, have values which depend strongly on μ and σ.

At the critical value μ_c, the limit cycle emerges, and consequently, for μ close to and above μ_c, its basin of attraction B_s (region of stability) is small compared to the one of the rest state, B_r. Also, there are dynamical effects as the speed on the limit cycle is not uniform but varies, so that the escape probability from B_s gets larger in regions that are traversed slowly. Therefore, relatively small noise can move the trajectory out of B_s, with only a small chance of moving back, since the rest state has a wider basin of attraction. For leaving the latter and moving back into B_s, a larger value of σ is needed. We have analyzed these effects in detail for a pair of coupled type I neurons in [29]. Thus, whether and where the trajectory when perturbed by noise leaves the basin of attraction of the limit cycle depends on the geometry of that basin and on the dynamics along the limit cycle, and therefore on the parameters controlling the dynamical system.

VI. DISCUSSION

We have seen that noise may terminate the spiking of a regularly firing HH neuron with varying degrees of efficacy when the mean input current μ is in the interval (μ_c,μ_c^*). Furthermore, a minimum in spike count may occur as a function of noise level. We found that this was the case for fixed (resting) initial conditions, for random initial conditions, and for a random time of switching on the noise. The fact that these results hold across a considerable variety of conditions, including both current and conductance based noise in single neurons, as demonstrated in the present paper, or in coupled neurons, of both Hodgkin-Huxley type (to be reported elsewhere) or of quadratic-integrate-and-fire type [27,29,30], lend support to the idea that these phenomena are of a general nature and may have a significant role in nervous system activity.

The above theory may be generalized to any system of nonlinear ordinary differential equations in which a stable limit cycle and a stable rest state coexist. Here, we have discussed one of many such systems describing neural spiking activity and we expect that the same principles will apply

even in the case of complex neuronal geometry. Experiments have already confirmed the inhibitory impact of noise on regularly spiking squid axons [33] where the effect of small noise on repetitive spiking was likened to a switch. Thus, one aspect of the functional significance of these effects of noise on rhythmic activity is that a very small disturbance can lead to a drastic change in neuronal behavior.

Since dynamical systems in diverse fields exhibit stable limit cycles coexisting with a stable rest state, we expect to find that the phenomena of inhibition of cyclic, repetitive, or rhythmic activity by noise and the occurrence of a minimum with increasing noise for certain parameter values will have widespread occurrence. Examples of fields where a stable limit cycle coexists with a stable rest state occur in circadian rhythms [44], cardiology [45], cell kinetics and tumor growth [46,47], oscillating neural networks [42,43], as well as in climatology, ecology, and astrophysics. We speculate that the phenomena we have demonstrated for the classical Hodgkin-Huxley model of spike generation can be analyzed in terms of a generic dynamical structure for this kind of system. Although the phenomena we have described are of interest in themselves, as indeed is stochastic resonance, their functional significance in neurobiological and other dynamical systems remains to be fully explored. We will discuss more fully the physiological significance of the above results in a longer publication.

APPENDIX

Here, we give the infinitesimal operator L^* for the six-component stochastic process in the conductance-based model. For notational convenience let $(t,\mathbf{y}) \equiv (t,y_1,y_2,y_3,y_4,y_5,y_6) \equiv (t,V,n,m,h,g_E,g_I)$ and let the vector of corresponding backward variables be $(s,\mathbf{x})$. Then (see, for example, [39]) the backward Kolmogorov equation for the transition probability density $p(\mathbf{y},t;\mathbf{x},s)$ is

$$-\frac{\partial p}{\partial s} = L^* p, \tag{12}$$

where L^* is the operator defined by

$$L^*p = \frac{1}{C}\{\bar{g}_K(V_K - x_1)x_2^4 + \bar{g}_{Na}(V_{Na} - x_1)x_3^3 x_4 + g_L(V_L - x_1) + x_5(V_E - x_1) + x_6(V_I - x_1)\}\frac{\partial p}{\partial x_1} + (\alpha_n(x_1)(1 - x_2) - \beta_n(x_1)x_2)\frac{\partial p}{\partial x_2}$$
$$+ (\alpha_m(x_1)(1 - x_3) - \beta_m(x_1)x_3)\frac{\partial p}{\partial x_3} + (\alpha_h(x_1)(1 - x_4) - \beta_h(x_1)x_4)\frac{\partial p}{\partial x_4} - \frac{1}{\tau_E}(x_5 - \bar{g}_E)\frac{\partial p}{\partial x_5} + \frac{\sigma_E^2}{2}\frac{\partial^2 p}{\partial x_5^2} - \frac{1}{\tau_I}(x_6 - \bar{g}_I)\frac{\partial p}{\partial x_6} + \frac{\sigma_I^2}{2}\frac{\partial^2 p}{\partial x_6^2}. \tag{13}$$

[1] E. M. Izhikevich, IEEE Trans. Neural Netw. **15**, 1063 (2004).
[2] B. Lindner, J. García-Ojalvo, A. Neiman, and L. Schimansky-Geier, Phys. Rep. **392**, 321 (2004).
[3] A. N. Burkitt, Biol. Cybern. **95**, 1 (2006).
[4] M. P. Nawrot, C. Boucsein, V. R. Molina, A. Riehle, A. Aertsen, and S. Rotter, J. Neurosci. Methods **169**, 374 (2008).
[5] A. Torcini, S. Luccioli, and T. Kreuz, Neurocomputing **70**, 1943 (2007).
[6] G. Deco and D. Marti, Biol. Cybern. **96**, 487 (2007).
[7] K. Diba, H. A. Lester, and C. Koch, J. Neurosci. **24**, 9723 (2004).
[8] S. Wang, F. Liu, W. Wang, and Y. Yu, Phys. Rev. E **69**, 011909 (2004).
[9] R. Meier, U. Egert, A. Aertsen, and M. P. Nawrot, Neural Networks **21**, 1085 (2008).
[10] D. J. MacGregor, C. K. I. Williams, and G. Leng, J. Neurosci. Methods **176**, 45 (2009).
[11] R. D. Vilela and B. Lindner, J. Theor. Biol. **257**, 90 (2009).
[12] D. K. Cope and H. C. Tuckwell, J. Theor. Biol. **80**, 1 (1979).
[13] X. Yu and E. R. Lewis, IEEE Trans. Biomed. Eng. **36**, 36 (1989).
[14] B. Lindner, A. Longtin, and A. Bulsara, Neural Comput. **15**, 1761 (2003).
[15] F. Y. M. Wan and H. C. Tuckwell, J. Theor. Neurobiol. **1**, 197 (1982).
[16] M. Barbi, A. Di Garbo, and F. Barbi, BioSystems **89**, 58 (2007).
[17] J. J. Collins, T. T. Imhoff, and P. Grigg, J. Neurophysiol. **76**, 642 (1996).
[18] A. Longtin, J. Stat. Phys. **70**, 309 (1993).
[19] F. Moss, L. M. Ward, and W. G. Sannita, Clin. Neurophysiol. **115**, 267 (2004).
[20] C. Nicolis, J. Stat. Phys. **70**, 3 (1993).
[21] G. Winterer *et al.*, Clin. Neurophysiol. **110**, 1193 (1999).
[22] F.-G. Zeng, Q.-J. Fu, and R. Morse, Brain Res. **869**, 251 (2000).
[23] Hu Gang, T. Ditzinger, C. Z. Ning, and H. Haken, Phys. Rev. Lett. **71**, 807 (1993).
[24] A. Longtin, P. W. Brouwer, and C. W. J. Beenakker, Phys. Rev. E **55**, 868 (1997).
[25] A. S. Pikovsky and J. Kurths, Phys. Rev. Lett. **78**, 775 (1997).
[26] G. Schmid, I. Goychuk, and P. Hänggi, Phys. Biol. **1**, 61 (2004).
[27] B. S. Gutkin, T. Hely, and J. Jost, Neurocomputing **58-60**, 753 (2004).
[28] S.-G. Lee, A. Neiman, and S. Kim, Phys. Rev. E **57**, 3292 (1998).
[29] B. S. Gutkin, J. Jost, and H. C. Tuckwell, EPL **81**, 20005

(2008).
[30] B. S. Gutkin, J. Jost, and H. C. Tuckwell, Theory Biosci. **127**, 135 (2008).
[31] A. L. Hodgkin, J. Physiol. (London) **107**, 165 (1948).
[32] B. S. Gutkin and G. B. Ermentrout, Neural Comput. **10**, 1047 (1998).
[33] D. Paydarfar, D. B. Forger, and J. R. Clay, J. Neurophysiol. **96**, 3338 (2006).
[34] A. L. Hodgkin and A. F. Huxley, J. Physiol. (London) **117**, 500 (1952).
[35] H. C. Tuckwell, J. Theor. Biol. **77**, 65 (1979).
[36] P. H. E. Tiesinga, J. V. Jose, and T. J. Sejnowski, Phys. Rev. E **62**, 8413 (2000).
[37] E. M. Izhikevich, Int. J. Bifurcation Chaos Appl. Sci. Eng. **10**, 1171 (2000).
[38] J. Jost, *Dynamical Systems* (Springer, Berlin, 2005).
[39] H. C. Tuckwell, *Stochastic Processes in the Neurosciences* (SIAM, Philadelphia, 1989).
[40] H. C. Tuckwell, J. Theor. Neurobiol. **5**, 87 (1986).
[41] H. C. Tuckwell, BioSystems **80**, 25 (2005).
[42] M. Steriade, Neuroscience **101**, 243 (2000).
[43] G. Buzsáki and A. Draguhn, Science **304**, 1926 (2004).
[44] M. E. Jewett and R. E. Kronauer, J. Theor. Biol. **192**, 455 (1998).
[45] *Computational Biology of the Heart*, edited by A. V. Panfilov and A. V. Holden (Wiley, New York, 1997).
[46] G. Lahav *et al.*, Nat. Genet. **36** 147 (2004).
[47] A. Goldbeter, Proc. Natl. Acad. Sci. U.S.A. **88**, 9107 (1991).